

PLANAR DISCRETE ISOTHERMIC NETS OF CONICAL TYPE

CHRISTIAN MÜLLER

ABSTRACT. We explore a specific discretization of isothermic nets in the plane which can also be interpreted as a discrete holomorphic map. The discrete orthogonality of the quadrilateral net is achieved by the so called conical condition imposed on vertex stars. That is, the sums of opposite angles between edges around all vertices are equal. This conical condition makes it possible to define a family of underlying circle patterns for which we can show invariance under Möbius transformations. Furthermore, we use the underlying circle pattern to characterize discrete isothermic nets in the projective model of Möbius geometry, and as Moutard nets in homogeneous coordinates in relation to the light cone in this model. We further investigate some examples of discrete isothermic nets and apply the Christoffel dual construction to obtain discrete minimal surfaces of conical type. Discrete differential geometry and conical nets and isothermic nets and minimal surfaces

1. INTRODUCTION AND PRELIMINARIES

1.1. **Introduction.** The focus of the present paper is the study of discrete isothermic nets in \mathbb{C} which in the smooth theory (assuming analyticity) are holomorphic. Various applications have brought up the need of developing mathematical methods to make complex analysis accessible to computational techniques. A very extensive source focusing on that aspect mainly using numerical methods to PDE problems is [10]. Another approach to discretize holomorphic maps can be made with circle packings. In that setting W.P. Thurston (1985) formulated a discrete version of the Riemann mapping theorem and conjectured convergence to the smooth theorem in the limit which was then proved in different ways by [9, 19]. A text book on the circle packing approach which also considers algorithmic issues is [21]. Another way of discretizing complex analysis is via circle patterns [3]. That is, the circles are not touching but intersecting in a meaningful way. There is also a notion of holomorphic maps in the theory of discrete integrable systems defined with the complex cross-ratio [2] or with orthogonal circle patterns [1].

In the present paper we study discrete isothermic nets represented by a quadrilateral net in \mathbb{C} , i.e., where all faces are quadrilaterals. In our case the property of discrete orthogonality is a condition defined on vertex stars rather than on faces. For reasons explained in Section 2 we call those type of isothermic nets to be of conical type.

E.B. Christoffel [6] constructs smooth isothermically parametrized minimal surfaces from isothermic parametrizations of the sphere. Here, *isothermic parametrization* means that the surface is parametrized by conformal curvature lines. Clearly, any curve on the sphere is a curvature line. Consequently, the property of isothermicity reduces to a

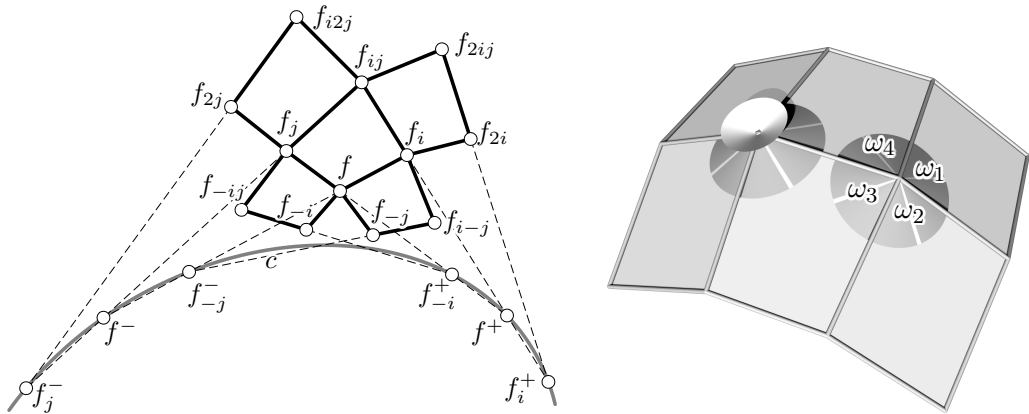


FIGURE 1. *Left:* Doliwa's definition [8] of Koenigs lattice. All six points of intersection f_{-i}^+ , f^+ , f_i^+ , f_{-j}^- , f^- , f_j^- of consecutive opposite edges lie on a conic c . *Right:* A conical net. All four quadrilaterals around each vertex touch a common cone of revolution.

conformally parametrized sphere. In the case where the parametrizations are analytic they correspond exactly to holomorphic maps on the Riemann sphere $\hat{\mathbb{C}} = \mathbb{C} \cup \{\infty\}$. Discrete versions of Christoffel's construction of minimal surfaces have already been considered thoroughly e.g., in [1–3, 11, 13, 15]. We apply this theory to construct discrete minimal surfaces of conical type.

1.2. Notation. Throughout the paper we are considering meshes with planar quadrilateral faces and with \mathbb{Z}^2 combinatorics. The vertices are located either in \mathbb{R}^n or in \mathbb{C} . The planarity condition in the latter case is clearly fulfilled automatically. We use the notions nets and meshes in an equivalent way and often denote those by their generating function, e.g., by $f : \mathbb{Z}^2 \rightarrow \mathbb{C}$. We are mainly considering local properties and therefore when we refer to one point of a net we use the notion f instead of $f(k, l)$ with $k, l \in \mathbb{Z}$. For the adjacent neighbors of f we use the subscripts mi or nj when we shift the first or second index by m or n , respectively. That is, $f_i = f(k + 1, l)$, $f_j = f(k, l + 1)$, $f_{ij} = f(k + 1, l + 1)$, $f_{-i} = f(k - 1, l)$, $f_{-j} = f(k, l - 1)$, $f_{2i} = f(k + 2, l)$, etc.

1.3. Discrete conjugate nets and Koenigs nets/lattices. Conjugate nets are objects of projective differential geometry since the characterizing properties are invariant under projective transformations. The commonly used discretization of two-dimensional conjugate nets are planar quadrilateral meshes, i.e., meshes where all faces are planar (see e.g., [3, 20]). Discrete conjugate nets enjoy popularity in theoretical and applied fields such as discrete differential geometry, computer graphics, architecture, etc.

Koenigs nets are special conjugate nets. In the following, we will consider two different discretizations of Koenigs nets [4, 8]. Both types of discretizations are invariant under projective transformations just like smooth Koenigs nets. This is the reason why most theorems of the present paper hold for both definitions (except in Section 4 where we need dualizability of the nets). We distinguish between them by using the respective author's own wordings: Koenigs nets [4] – Koenigs lattice [8].

Koenigs nets. First, there is the definition by A.I. Bobenko and Yu.B. Suris [4] focusing on the dualization property. Conjugate nets $f : \mathbb{Z}^2 \rightarrow \mathbb{R}^n$ are called *Koenigs*

nets if they allow for Christoffel dualization, i.e., if there is a real valued function $\nu : \mathbb{Z}^2 \rightarrow \mathbb{R} \setminus \{0\}$ and a net $f^* : \mathbb{Z}^2 \rightarrow \mathbb{R}^3$ such that $\nu_{ij} : \nu = (M - f_{ij}) : (M - f)$ and $\nu_j : \nu_i = (M - f_j) : (M - f_i)$, where M is the intersection point of the diagonals of the quadrilateral f, f_i, f_{ij}, f_j and such that

$$(1) \quad f_i^* - f^* = \frac{f_i - f}{\nu\nu_i} \quad \text{and} \quad f_j^* - f^* = -\frac{f_j - f}{\nu\nu_j}$$

hold. Then f^* is determined up to translation and scaling and f^* is called *dual* of f . As it turns out (see [4]) it is possible to characterize the Koenigs property in terms of so called *exact discrete multiplicative one-forms* as follows. Let q be the function defined on the diagonals representing ratios of the form $(f - M) : (f_{ij} - M)$. Then f is a Koenigs net if and only if q is an exact multiplicative one-form meaning that the product of all values of q along any cycle of diagonals equals 1.

Koenigs lattices. Second, there is A. Doliwa's [8] definition. Here, we need to consider a face $F = (f, f_i, f_{ij}, f_j)$ and its four edgewise neighboring faces. Then we intersect opposite (extended) edges of three consecutive quadrilaterals in a row and in a column as illustrated by Figure 1 (left) to obtain the following six points

$$\begin{aligned} f_{-i}^+ &:= (f_{-i} \vee f_{-ij}) \cap (f \vee f_j), & f_{-j}^- &:= (f_{-j} \vee f_{i-j}) \cap (f \vee f_i), \\ f^+ &:= (f \vee f_j) \cap (f_i \vee f_{ij}), & f^- &:= (f \vee f_i) \cap (f_j \vee f_{ij}), \\ f_i^+ &:= (f_i \vee f_{ij}) \cap (f_{2i} \vee f_{2ij}), & f_j^- &:= (f_j \vee f_{ij}) \cap (f_{2j} \vee f_{2ij}), \end{aligned}$$

where $a \vee b$ denotes the straight line connecting points a and b . Then a conjugate net $f : \mathbb{Z}^2 \rightarrow \mathbb{R}^n$ is called a *Koenigs lattice* if the six just defined vertices $f_{-i}^+, f^+, f_i^+, f_{-j}^-, f^-, f_j^-$ lie on a conic (see Figure 1 left). This is indeed a condition since five different points already uniquely determine a conic.

REMARK 1. *Most results of the present paper can be formulated and proved for both notions, Koenigs nets and lattices. Note in this regard that a remark in [4] says that the intersection points $M : \mathbb{Z}^2 \rightarrow \mathbb{R}^n$ of the diagonals of a Koenigs net f constitute a Koenigs lattice. Nevertheless, as we will explain later (in Remark 14), we do have to consider both notions independently.*

2. DISCRETE ISOTHERMIC NETS IN \mathbb{C}

In this section we first give a motivation for our definition of discrete isothermic nets. Then we present characterizations and properties by looking at different models of Möbius geometry.

2.1. Motivation and definition. Among different approaches to discrete curvature lines we focus on so called conical nets [12]. *Conical nets* are quadrilateral meshes with planar faces such that all faces around one vertex are tangent to a cone of revolution (see Figure 1 right).

The reason why it is sensible to call conical nets discrete curvature line parametrizations is the following. Geometrically speaking the axes of the cones of revolution corresponding to two adjacent vertices of a conical net are intersecting. In other words the discrete normals along a discrete parameter curve form a discrete developable surface. Now we recall the analogous fact in smooth differential geometry where curvature

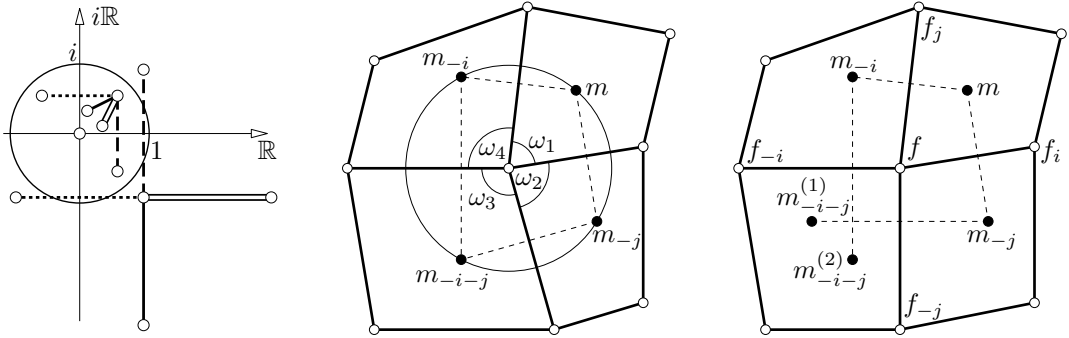


FIGURE 2. *Left:* The Möbius transformation $z \mapsto 1/z$ applied to (the vertices of) a vertex star. Note that the sum of opposite angles is *not* preserved. *Center:* A vertex star fulfilling the angle condition (2). In this case reflecting a point m in the edges is independent of the path, i.e., $m_{-i-j}^{(1)} = m_{-i-j}^{(2)} = m_{-i-j}$. The four points $m, m_{-i}, m_{-j}, m_{-i-j}$ are concircular. *Right:* A vertex star of a net in \mathbb{C} not fulfilling the angle condition (2). In this case reflecting a point m in the edges is not independent of the path, i.e., $m_{-i-j}^{(1)} \neq m_{-i-j}^{(2)}$.

lines are characterized by the fact that the surface normals along those curves form developable surfaces if and only if the curves are curvature lines. Consequently, we regard polygons of the form $f(\mathbb{Z}, k)$ or $f(k, \mathbb{Z})$ (which are discrete parameter curves) of a conical net as discrete curvature lines [3, 12].

Conical nets as a special type of polyhedral surfaces were invented for applications in architecture [12] because those meshes resemble smooth curvature line nets (and therefore orthogonal nets), and in addition allow for so called face offsets that can be used as a support structure. In terms of elementary geometry conical meshes are characterized by equality of opposite angle sums at all vertices. To be more precise, let us consider a vertex of valence four in the generic case where the vertex star is not contained in a plane. Further, let $\omega_1, \dots, \omega_4$ measure the angles between the edges of the four quadrilaterals around the vertex in cyclic order (see Figure 1 right and Figure 2 center). Then this vertex is conical if and only if

$$(2) \quad \omega_1 + \omega_3 = \omega_2 + \omega_4.$$

Clearly, equivalence here is only guaranteed for non-planar vertex stars. For a proof of this characterization and further details see [17, 22].

In analogy to [3, Def. 4.20] we add the Koenigs property to a discrete curvature line net to obtain isothermicity.

DEFINITION 2. A (discrete) isothermic net/lattice (of conical type) $f : \mathbb{Z}^2 \rightarrow \mathbb{R}^3$ is a conical Koenigs net/lattice.

Our main focus does not lie in *spatial* discrete isothermic surfaces except for some examples of discrete minimal surfaces in Section 4 but rather on discrete isothermic nets/lattices in \mathbb{C} . The property of having a cone of revolution tangent to all faces at each vertex is fulfilled by any net in a plane. To overcome that problem we replace the “cone-condition” by the (in the non-planar case) equivalent angle condition (2). We thus arrive at our main definition.

DEFINITION 3. A (discrete) isothermic net/lattice (of conical type) $f : \mathbb{Z}^2 \rightarrow \mathbb{C}$ is a Koenigs net/lattice which fulfills the angle condition (2) at all vertex stars.

REMARK 4. In our planar situation we additionally have the property that the sum of all angles at one vertex equals 2π , i.e., $\omega_1 + \dots + \omega_4 = 2\pi$. Thus, our angle condition (2) immediately turns into $\omega_1 + \omega_3 = \omega_2 + \omega_4 = \pi$.

There is one thing we would like to expect from any definition of discrete isothermic nets/lattices. It is invariance under Möbius transformations. For example in [2] they call a map $f : \mathbb{Z}^2 \rightarrow \mathbb{C}$ discrete isothermic (or discrete holomorphic) if the cross-ratio equals -1 for all quadrilaterals f, f_i, f_{ij}, f_j , i.e., if $\text{cr}(f, f_i, f_{ij}, f_j) = (f - f_i)(f_i - f_{ij})^{-1}(f_{ij} - f_j)(f_j - f)^{-1} = -1$. Since the cross-ratio is invariant under Möbius transformations the notion of holomorphicity from [2] is invariant under Möbius transformations applied to all vertices of the net. However, Figure 2 (left) illustrates that applying a Möbius transformation directly to the vertices would destroy the characterizing properties (in Figure 2 (left) obviously the conical condition is destroyed). Nevertheless, there is a way to apply Möbius transformations to discrete isothermic nets/lattices and retain the properties of Definition 3. We will elaborate on that in Section 2.5 after introducing the notion of an underlying circle pattern.

2.2. The underlying family of circle patterns. Let us consider a discrete isothermic net of conical type $f : \mathbb{Z}^2 \rightarrow \mathbb{C}$ and a point $m \in \mathbb{C}$. We reflect m in the supporting straight lines carrying ff_i and ff_j to obtain m_{-j} and m_{-i} , respectively. For an illustration see Figure 2 (right). Then we reflect m_{-i} in ff_i and m_{-j} in ff_{-j} to obtain $m_{-i-j}^{(1)}$ and $m_{-i-j}^{(2)}$, respectively. The question whether or not the last two points coincide is answered by the following lemma which is also true in the non-planar setting, i.e., for conical nets in \mathbb{R}^3 [17].

LEMMA 5. For any quadrilateral net in \mathbb{C} fulfilling (2) and in particular for discrete isothermic nets/lattices of conical type we have

$$m_{-i-j}^{(1)} = m_{-i-j}^{(2)} =: m_{-i-j}.$$

Proof. For the following geometric proof cf. Figure 2 (center and right). Reflecting a point on two intersecting lines enclosing an angle of α is equivalent to rotating the point about 2α around the point of intersection. Thus, $m_{-i-j}^{(1)}$ is equivalently generated by a rotation about an angle of $2\omega_2$ which is $2\pi - 2\omega_4$ according to Remark 4. In other words we obtain $m_{-i-j}^{(1)}$ also by rotating m about an angle of $2\pi - 2\omega_4$ in the other direction which is exactly how we got $m_{-i-j}^{(2)}$. \square

In this way we can assign a unique point m_F to each face F around a vertex f of a discrete isothermic net/lattice $f : \mathbb{Z}^2 \rightarrow \mathbb{C}$ once we have chosen m . Due to the construction of the four points $m, m_{-i}, m_{-i-j}, m_{-j}$ through reflections those points are concircular with center f (see also Figure 2 center). As we now continue to reflect m_F in the four edges corresponding to F we obtain a circular quadrilateral net $m : (\mathbb{Z}^2)^* \rightarrow \mathbb{C}$, where $(\mathbb{Z}^2)^*$ denotes the dual graph of \mathbb{Z}^2 . We identify $(\mathbb{Z}^2)^*$ and \mathbb{Z}^2 in the following since they have the same combinatorics. We call the two parameter family of quadrilateral nets $m(\mathbb{Z}^2)$ *underlying family of circular quadrilateral nets* or focusing on the corresponding

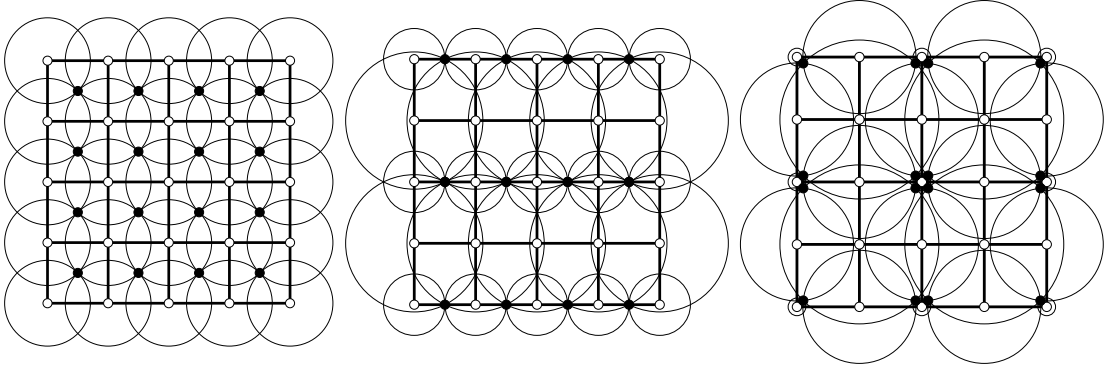


FIGURE 3. Different underlying circle patterns of the same discrete isothermic net/lattice $f : \mathbb{Z}^2 \rightarrow \mathbb{C}$. A stereographic projection as well as their Christoffel duals are illustrated by Figure 10.

circles $s : \mathbb{Z}^2 \rightarrow \{\text{circles} \subset \mathbb{C}\}$ underlying family of circle patterns. Three different instances of underlying circle patterns of the same net $f(\mathbb{Z}^2)$ are depicted in Figure 3. The following remark states that we can also go the other way around.

REMARK 6. *If we start with four concircular points then the mirror axes of two consecutive points all pass through the given circle center and form a planar vertex star fulfilling the angle condition (2). Thus, the centers $f : \mathbb{Z}^2 \rightarrow \mathbb{C}$ of a circle pattern with \mathbb{Z}^2 combinatorics determines a quadrilateral net in \mathbb{C} which meets the angle condition (2) in all vertices.*

2.3. Representation of circles by points. To work with the underlying circle pattern we choose to take advantage of point models of circles. In the following we recall three models and their relations.

2.3.1. *Paraboloid model.* Any circle s in \mathbb{C} with center c and radius r can be represented by the point

$$s^p = (c, |c|^2 - r^2) \in \mathbb{C} \times \mathbb{R} \cong \mathbb{R}^3.$$

Geometrically, we obtain this point by the following procedure. We project the circle in z -direction to the paraboloid $x^2 + y^2 - z = 0$. The curve of intersection is an ellipse and the pole of the supporting plane of this ellipse with respect to the paraboloid is exactly our representative s^p . Consequently, it is called *paraboloid model* or *isotropic model* (see e.g., [16] for a justification of the latter name).

2.3.2. *Spherical model.* We stereographically project the circle s to the unit sphere. Here, we restrict ourselves to the case where the projected circles are no great circles. Then we construct the pole with respect to the unit sphere which reads

$$(3) \quad \phi(s) = (2c, |c|^2 - r^2 - 1) / (|c|^2 - r^2 + 1) \in \mathbb{C} \times \mathbb{R} \cong \mathbb{R}^3.$$

We obtain the spherical model by applying a special projective transformation to the paraboloid model that maps the paraboloid to the unit sphere.

2.3.3. *Projective model.* Circles s in \mathbb{C} are represented in the *projective model* $\mathbb{P}(\mathbb{R}^{3,1})$ by homogeneous coordinates

$$\hat{s} = \left(c, \frac{1}{2}(|c|^2 - r^2 - 1), \frac{1}{2}(|c|^2 - r^2 + 1) \right) \in \mathbb{C} \times \mathbb{R}^2 \cong \mathbb{R}^{3,1}.$$

Here, $\mathbb{R}^{3,1}$ denotes the Minkowski space with an inner product $\langle \cdot, \cdot \rangle_1$ of signature $(+++-)$. For further details on projective models of Möbius geometry see e.g., [3, 5, 11]. Proper circles s , i.e., circles with non-vanishing radius, are characterized by $\langle \hat{s}, \hat{s} \rangle_1 > 0$, whereas points are lifted to the *light cone* $\mathbb{L}^{3,1} = \{\hat{x} \in \mathbb{R}^{3,1} \mid \langle \hat{x}, \hat{x} \rangle_1 = 0\}$. Two circles s_1, s_2 are intersecting orthogonally if and only if their representing points are lying polar with respect to the light cone, i.e., $\langle \hat{s}_1, \hat{s}_2 \rangle = 0$. A pencil of circles in \mathbb{C} is represented by a straight line in $\mathbb{R}^{3,1}$. The representatives \hat{s} of circles lie in the affine hyperplane $x_4 - x_3 = 1$. For a schematic illustration of the projective model and the light cone see Figure 4 (left). We immediately see that the linear map

$$(4) \quad (x_1, \dots, x_4) \mapsto (x_1, x_2, (x_3 - x_4)/2, (x_3 + x_4)/2)$$

maps the paraboloid model $(s^p, 1)$ (lifted to the hyperplane $x_4 = 1$) to the projective model $\phi(s)$.

2.4. Discrete isothermic nets/lattices in point models. The goal of this paragraph is to establish bijective relations between an underlying circle pattern of a discrete isothermic net/lattice (of conical type) and special types of nets in the point models of circles.

LEMMA 7. *Let s_1, s_2, s_3 denote three circles of a pencil of circles with centers c_1, c_2, c_3 such that $c_3 = (1 - \lambda)c_1 + \lambda c_2$ for some $\lambda \in \mathbb{R}$. Then*

$$s_3^p = (1 - \lambda)s_1^p + \lambda s_2^p \quad \text{and} \quad \hat{s}_3 = (1 - \lambda)\hat{s}_1 + \lambda \hat{s}_2.$$

Thus, the representatives of three circles of a pencil in the paraboloid and projective models are collinear and their affine ratio equals the ratio of their corresponding centers.

Proof. It is easily verified and well known that a pencil of circles is represented by a line in the paraboloid model. Further, by definition s^p lies in x_3 -direction over the center of s . Consequently, the first equation is clear. The second equation is then also clear since the linear map (4) maps the three points s_i^p to \hat{s}_i . \square

LEMMA 8. *Let s_1, \dots, s_4 be four circles in \mathbb{C} all passing through one point m . Then $\hat{s}_1, \dots, \hat{s}_4$ are coplanar and the supporting plane is contained in the tangent space of the light cone at \hat{m} .*

Proof. Lemma 7 immediately implies that in the paraboloid model circles s passing through a point m are mapped to points in the tangent plane of the paraboloid at m^p . Consequently, s_1^p, \dots, s_4^p are coplanar. The linear map (4) maps the tangent plane of the paraboloid to a two dimensional plane P in the tangent space of the light cone $T_{\hat{m}}\mathbb{L}^{3,1}$. Thus, P is the supporting plane of $\hat{s}_1, \dots, \hat{s}_4$. \square

With these preparations we can prove the following characterization of (discrete) isothermic nets/lattices of conical type in the projective model.

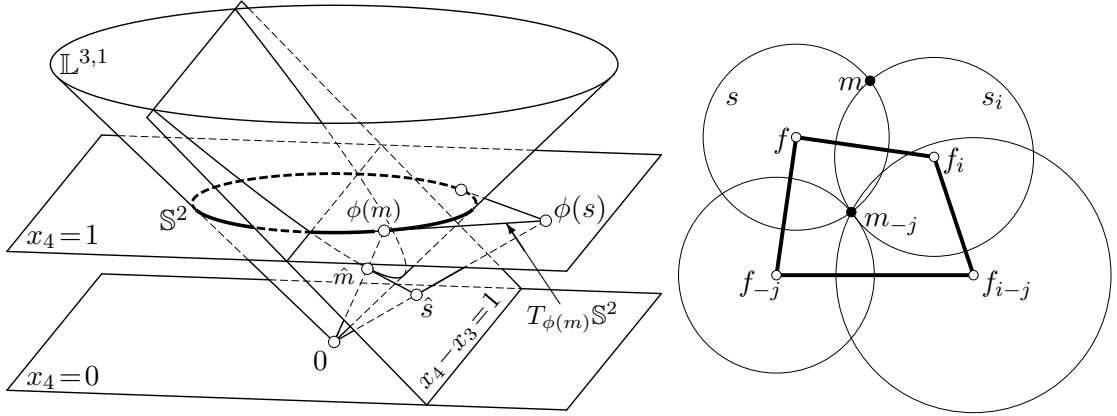


FIGURE 4. *Left:* A schematic illustration of the generation of the projective model of Möbius geometry. A point $m \in \mathbb{C}$ is stereographically projected to the sphere $\phi(m) \in \mathbb{S}^2$. Here \mathbb{S}^2 is depicted as a circle. \mathbb{S}^2 is embedded in the affine hyperplane $x_4 = 1$ and then projected to the affine hyperplane $x_4 - x_3 = 1$ to obtain the homogeneous coordinate representation \hat{m} . A circle $s \in \mathbb{C}$ is stereographically projected to a circle on \mathbb{S}^2 . $\phi(s)$ is the pole of the plane which carries this circle. A central projection with center 0 maps $\phi(s)$ to \hat{s} in the affine hyperplane $x_4 - x_3 = 1$. \hat{s} is the representative of the circle in the projective model. *Right:* A planar face $\hat{s}, \hat{s}_i, \hat{s}_{i-j}, \hat{s}_{-j}$ in the tangent space of the light cone at \hat{m}_{-j} represents four circles which meet in a point m_{-j} .

THEOREM 9. (a) *Let $f : \mathbb{Z}^2 \rightarrow \mathbb{C}$ be a discrete isothermic net/lattice of conical type and let $s : \mathbb{Z}^2 \rightarrow \{\text{circles} \subset \mathbb{C}\}$ be an underlying circle pattern. Then the lift to the projective model $\hat{s} : \mathbb{Z}^2 \rightarrow \mathbb{R}^{3,1}$ is a Koenigs net/lattice where each face is contained in a tangent space of the light cone.*
 (b) *Let $\hat{s} : \mathbb{Z}^2 \rightarrow \{\hat{x} \in \mathbb{R}^{3,1} \mid \langle \hat{x}, \hat{x} \rangle_1 \geq 0\}$ be a discrete Koenigs net/lattice where each face is contained in a tangent space of the light cone. Then the centers $f : \mathbb{Z}^2 \rightarrow \mathbb{C}$ of the corresponding circles $s : \mathbb{Z}^2 \rightarrow \{\text{circles} \subset \mathbb{C}\}$ form a discrete isothermic net/lattice of conical type.*

Proof. To verify (a) we have to show planarity of the faces of $\hat{s}(\mathbb{Z}^2)$ and the Koenigs properties.

By construction of the underlying circle pattern $s : \mathbb{Z}^2 \rightarrow \{\text{circles} \subset \mathbb{C}\}$ all four circles s, s_i, s_{i-j}, s_{-j} corresponding to a face of f are intersecting in one point m . Thus, Lemma 8 yields coplanarity of the lifted representatives $\hat{s}, \hat{s}_i, \hat{s}_{i-j}, \hat{s}_{-j}$ of the four circles under consideration and the supporting plane is contained in the tangent space $T_{\hat{m}}\mathbb{L}^{3,1}$ of the light cone at \hat{m} .

Regarding the Koenigs properties we need to consider both cases, net/lattice, separately. It is clear that either type of the Koenigs property in the definition of isothermic nets/lattices survives the transformation from \mathbb{C} to the parabolic model. Because, for Koenigs lattices we realize that the net $s^p : \mathbb{Z}^2 \rightarrow \mathbb{R}^3$ in the paraboloid model has planar faces and that the orthogonal projection back to the x_1x_2 -plane is the original net $f : \mathbb{Z}^2 \rightarrow \mathbb{C}$. Consequently, we obtain a conic through $s_{-i}^{p+}, s^{p+}, s_i^{p+}, s_{-j}^{p-}, s^{p-}, s_j^{p-}$ by projecting the existing conic through $f_{-i}^+, f^+, f_i^+, f_{-j}^-, f^-, f_j^-$ up to the plane $(s^p, s_i^p, s_{ij}^p, s_j^p)$. Afterwards, the linear map (4) maps the conic to $\mathbb{R}^{3,1}$.

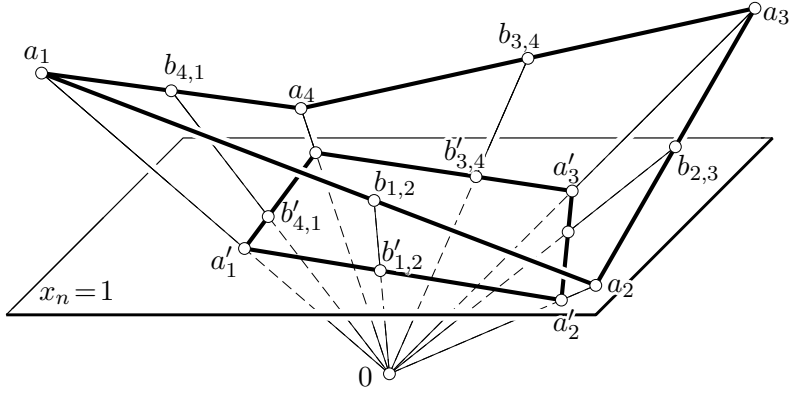


FIGURE 5. A central projection of a closed non-planar polygon a_1, \dots, a_k in \mathbb{R}^n (here $k = 4$) to an affine hyperplane. Proposition 10 implies that the products of lengths ratios of all line segments $a_i, b_{i,i+1}, a_{i+1}$ are the same for both polygons, the original one with vertices a_i and the projected one with vertices a'_i .

For Koenigs nets, Lemma 7 implies that the ratio of diagonal segments of the representatives s^p, d^p, s_{ij}^p is the same as the ratio of the corresponding diagonal segments of the diagonal f, f_{ij} , where d is the point of intersection of the diagonals of the considered face. Since the linear map (4) keeps affine ratios also the lift to the projective model is a net where the ratios of diagonal segments constitute an exact discrete multiplicative one-form, and thus it is a Koenigs net.

We use a similar argument to verify (b). If $\hat{s} : \mathbb{Z}^2 \rightarrow \mathbb{R}^{3,1}$ is a Koenigs net/lattice then the inverse of (4) maps the net/lattice to the parabolic model where conics are mapped to conics and affine ratios of diagonal segments are preserved. Afterwards, the orthogonal projection to the x_1x_2 -plane also maps conics to conics and preserves affine ratios. Consequently, the Koenigs property survives for both types.

It remains to verify the angle condition (2) for all vertex stars of f . Each face of $\hat{s}(\mathbb{Z}^2)$ is contained in some $T_{\hat{m}}\mathbb{L}^{3,1}$, i.e., in the tangent space of the light cone at some point \hat{m} . Thus, each point in such a face represents a circle passing through m which is the point represented by \hat{m} . Since two adjacent vertices \hat{s}, \hat{s}_i of the net/lattice $\hat{s}(\mathbb{Z}^2)$ are incident with two adjacent faces the two corresponding circles s, s_i intersect in two points m, m_{-j} (see Figure 4 right). Consequently, Remark 6 implies that the centers f of the circles represented by \hat{s} is a net/lattice that meets the angle condition (2). \square

The following proposition generalizes [3, Thm. 9.11] which says that the cyclic product of directed lengths ratios is invariant under projective transformations. This result is still true if we replace projective transformations by central projections to hyperplanes.

PROPOSITION 10. *Let $a_1, \dots, a_k \in \mathbb{R}^n$ with $k \geq 3$ and let $b_{i,i+1}$ be a point on the straight line $a_i \vee a_{i+1}$ with $b_{i,i+1} = (1 - \lambda_i)a_i + \lambda_i a_{i+1}$. Then the product of oriented lengths ratios*

$$\prod_{i=1}^k \frac{b_{i,i+1} - a_i}{b_{i,i+1} - a_{i+1}}$$

is invariant under those central projections to hyperplanes (see Figure 5) which do not send any of the considered points to infinity nor map a line segment to a point.

Proof. W.l.o.g. we project to the hyperplane $x_n = 1$ with center 0. We consider the three points a, b, c on a line and its projections a', b', c' which are given by

$$a' = \frac{1}{a^n}a = \frac{1}{a^n}(a^1, \dots, a^n) = (a^1/a^n, \dots, a^{n-1}/a^n, 1),$$

and analogously for b' and c' . There are $\lambda, \mu \in \mathbb{R}$ with $c = (1 - \lambda)a + \lambda b$ and $c' = (1 - \mu)a' + \mu b'$. Consequently,

$$\frac{1}{(1 - \lambda)a^n + \lambda b^n}((1 - \lambda)a + \lambda b) = (1 - \mu)\frac{1}{a^n}a + \mu\frac{1}{b^n}b,$$

and thus

$$\frac{\mu}{\mu - 1} = \frac{\lambda b^n}{(\lambda - 1)a^n}.$$

For the product of lengths ratios we therefore obtain by canceling all a_i^n

$$\prod_{i=1}^k \frac{\mu_i}{\mu_i - 1} = \frac{\lambda_1 a_2^n}{(\lambda_1 - 1)a_1^n} \cdot \frac{\lambda_2 a_3^n}{(\lambda_2 - 1)a_2^n} \cdot \dots \cdot \frac{\lambda_k a_1^n}{(\lambda_k - 1)a_k^n} = \prod_{i=1}^k \frac{\lambda_i}{\lambda_i - 1}.$$

Thus, we get

$$\prod_{i=1}^k \frac{b_{i,i+1} - a_i}{b_{i,i+1} - a_{i+1}} = \prod_{i=1}^k \frac{\lambda_i}{\lambda_i - 1} = \prod_{i=1}^k \frac{\mu_i}{\mu_i - 1} = \prod_{i=1}^k \frac{b'_{i,i+1} - a'_i}{b'_{i,i+1} - a'_{i+1}},$$

which concludes the proof. \square

COROLLARY 11. *Any lift $\mu\hat{s} : \mathbb{Z}^2 \rightarrow \mathbb{R}^{3,1}$ of an underlying circle pattern of a discrete isothermic net/lattice which is still a net with planar faces for some function $\mu : \mathbb{Z}^2 \rightarrow \mathbb{R} \setminus \{0\}$ is a discrete Koenigs net/lattice.*

Proof. For Koenigs nets Proposition 10 implies that the product of a cycle of diagonal segments does not change when multiplying each vector of homogeneous coordinates \hat{s} by an individual scalar μ . Consequently, the discrete multiplicative one form defined as ratios of diagonal segments is exact for all possible lifts of the form $\mu\hat{s} : \mathbb{Z}^2 \rightarrow \mathbb{R}^{3,1}$, or for none. Since Theorem 9(a) implies that there is at least one lift, namely \hat{s} , which is a Koenigs net, all possible lifts of the form $\mu\hat{s}$ which have planar faces are Koenigs nets.

As for the Koenigs lattices we have that the six points lying on the characterizing conic for the face (f, f_i, f_{ij}, f_j) are mapped by a central projection to six points on the projected conic into the plane of the face $(\mu f, \mu_i f_i, \mu_{ij} f_{ij}, \mu_j f_j)$. \square

COROLLARY 12. (a) *Let $f : \mathbb{Z}^2 \rightarrow \mathbb{C}$ be a discrete isothermic net/lattice of conical type and let $s : \mathbb{Z}^2 \rightarrow \{\text{circles} \subset \mathbb{C}\}$ be an underlying circle pattern. Then $\phi(s) : \mathbb{Z}^2 \rightarrow \mathbb{R}^3$ is a discrete isothermic net/lattice, i.e., a conical Koenigs net/lattice.*

(b) *Let $\tilde{s} : \mathbb{Z}^2 \rightarrow \mathbb{R}^3$ be a conical Koenigs net/lattice where all faces touch the unit sphere. Then the centers of the circle pattern $\phi^{-1}(\tilde{s})$ form a discrete isothermic net/lattice of conical type.*

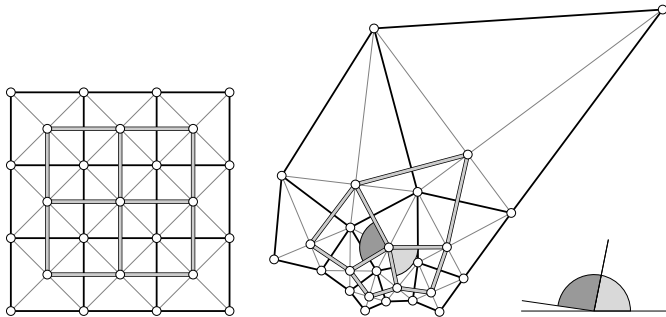


FIGURE 6. We obtain the discrete isothermic net \tilde{f} (center; single line net) after applying a Möbius transformation to the canonical underlying circle pattern of the \mathbb{Z}^2 net f (left) as in Thm. 13. Note that the net \tilde{M} (center; double line) consisting of the intersection points of the diagonals is no longer conical because opposite angles do *not* sum up to π (see also Remark 14).

Proof. This is an immediate consequence of Corollary 11 and the fact that the net/lattice $\phi(\mathbb{Z}^2)$ in the spherical model is that special lift $\mu\hat{s}(\mathbb{Z}^2)$ which lives in the hyperplane $x_4 = 1$. \square

2.5. Discrete isothermic nets and Möbius transformations. We already saw (Figure 2 left) that we cannot apply a Möbius transformation to the vertices of a discrete isothermic net/lattice of conical type without destroying isothermicity. However, we can apply Möbius transformations to the underlying circle pattern and retain the property of isothermicity.

THEOREM 13. *Let $f : \mathbb{Z}^2 \rightarrow \mathbb{C}$ be a discrete isothermic net/lattice of conical type and let $s : \mathbb{Z}^2 \rightarrow \{\text{circles} \subset \mathbb{C}\}$ be an underlying circle pattern. Furthermore, let M be a Möbius transformation. Then the centers of the circle pattern $M \circ s(\mathbb{Z}^2)$ form a discrete isothermic net/lattice of conical type.*

Proof. By applying Theorem 9(a) we obtain that the image of the circle pattern $s(\mathbb{Z}^2)$ in the projective model is a Koenigs net/lattice where each face is contained in a tangent space of the light cone. The fundamental theorem of Möbius geometry implies that the Möbius transformation M acts in the projective model $\mathbb{P}(\mathbb{R}^{3,1})$ as projective transformation which preserves the light cone. The property of being a Koenigs net/lattice is invariant under projective transformations. Thus, the transformed net/lattice is again a conical Koenigs net/lattice where all faces are contained in a tangent space of the light cone. Consequently, Theorem 9(b) implies that the centers of $M \circ s(\mathbb{Z}^2)$ form a discrete isothermic net/lattice of conical type. \square

REMARK 14. *As mentioned before the intersection points M of the diagonals of a discrete isothermic net f (i.e., in the sense of [4]) constitute a Koenigs lattice (i.e., in the sense of [8]). Applying a Möbius transformation as stated in Theorem 13 to f yields another isothermic net \tilde{f} with a corresponding net \tilde{M} . However, \tilde{M} is no longer guaranteed to be an isothermic lattice (not even conical) even if M was. This can easily be verified by a counterexample (see Figure 6).*

2.6. Moutard nets. Darboux [7] showed the characterization of (smooth) isothermic surfaces in terms of Moutard nets in the light cone. A *Moutard net* is a parametrization f of a surface which fulfills the PDE $f_{xy} = af$ for some function a . A discrete version of this relation in the setting of circular nets can be found in [4, Th. 4.12]. In our conical

setting we obtain a similar characterization. Note that in this section our objects are Koenigs nets (i.e., in the sense of [4]).

THEOREM 15. *Let $f : \mathbb{Z}^2 \rightarrow \mathbb{C}$ be a discrete isothermic net of conical, and let $s : \mathbb{Z}^2 \rightarrow \{\text{circles} \subset \mathbb{C}\}$ be an underlying circle pattern. Further, let ν be the real valued function defined for Koenigs nets (see Section 1.3). Then the special lift $y := \nu^{-1}\hat{s} : \mathbb{Z}^2 \rightarrow \mathbb{R}^{3,1}$ of the circles to a net with faces tangent to the light cone fulfills the discrete Moutard equation with minus signs*

$$y_{ij} - y = a_{ij}(y_j - y_i),$$

where $a_{ij} = (\nu_{ij}^{-1} - \nu^{-1})/(\nu_j^{-1} - \nu_i^{-1})$.

Conversely, any net $y : \mathbb{Z}^2 \rightarrow \mathbb{R}^{3,1}$ with faces tangent to the light cone and fulfilling the Moutard equation represents a circle pattern in \mathbb{C} whose centers represent a discrete isothermic net of conical type.

Proof. Let us first recall the following theorem by A.I. Bobenko and Yu.B. Suris [4, Thm. 3.15]. It says that a net $g : \mathbb{Z}^2 \rightarrow \mathbb{R}^n$ is a Koenigs net (and especially has planar faces) if and only if there is a function $\nu : \mathbb{Z}^2 \rightarrow \mathbb{R} \setminus \{0\}$ which is defined for dualizing g (as described in Section 1.3) such that the following discrete Moutard equation is fulfilled

$$(5) \quad \nu_{ij}^{-1}(g_{ij}, 1) - \nu^{-1}(g, 1) = a_{ij}(\nu_j^{-1}(g_j, 1) - \nu_i^{-1}(g_i, 1)).$$

In our setting Theorem 9(a) implies that $\hat{s}(\mathbb{Z}^2)$ is a Koenigs net with faces tangent to the light cone. Consequently, by using $\hat{s} : \mathbb{Z}^2 \rightarrow \mathbb{R}^{3,1}$ for g in Equation (5) and by setting $y := \nu^{-1}\hat{s}$ Equation (5) turns into

$$(y_{ij}, \nu_{ij}^{-1}) - (y, \nu^{-1}) = a_{ij}((y_j, \nu_j^{-1}) - (y_i, \nu_i^{-1})).$$

The first component (actually the first four components) of the last equation is exactly the Moutard equation $y_{ij} - y = a_{ij}(y_j - y_i)$. The faces of the Moutard net $y : \mathbb{Z}^2 \rightarrow \mathbb{R}^{3,1}$ are still tangent to the light cone.

The other direction follows immediately from Theorem 9(b) and the characterization of Koenigs nets via the discrete Moutard equation (5). \square

3. EXAMPLES

As mentioned before analytic isothermic nets in \mathbb{C} are holomorphic. In this section we discuss discretizations of elementary holomorphic maps. All examples except the last one are isothermic nets and isothermic lattices simultaneously which leads us to call those nets/lattices simply discrete holomorphic. before we apply the Christoffel dual construction to isothermic nets to obtain minimal surfaces in Section 4.

3.1. Discrete identity map. The *discrete identity map* $f : \mathbb{Z}^2 \rightarrow \mathbb{C}$ with $(k, l) \mapsto k + il$ (where $i = \sqrt{-1}$) is obviously a discrete holomorphic map (of conical type). $f(\mathbb{Z}^2)$ is illustrated by Figure 3 with three different underlying circle patterns. We can reparametrize f in the form $(k, l) \mapsto \alpha(k) + i\beta(l)$, where $\alpha, \beta : \mathbb{Z} \rightarrow \mathbb{R}$ are either strictly monotonically increasing or decreasing and still keep holomorphicity. Additionally, this type of net is circular, i.e., in the case of $\alpha = \beta = \text{const.}$ it is also discrete holomorphic in the sense of [2].

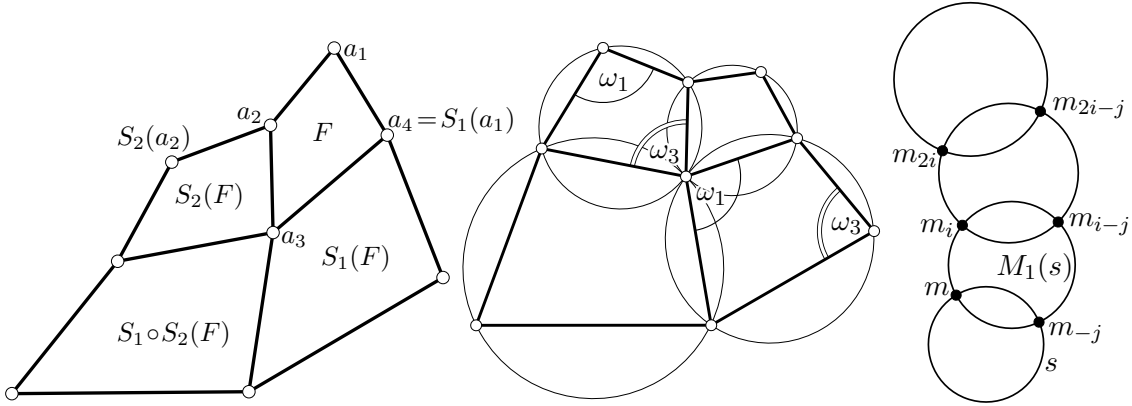


FIGURE 7. *Left:* Two similarities S_1, S_2 , each mapping an edge of a quadrilateral a_1, \dots, a_4 to the opposite edge are commuting (see Lemma 16). Applying this similarities yields a quadrilateral net/lattice $S_1^k \circ S_2^l(a_1)$ (locally) without gaps. *Center:* Circular quadrilateral net/lattice constructed with similarities. The circularity condition implies $\omega_1 + \omega_3 = \pi$. Thus, here the angle condition (2) is fulfilled. *Right:* A given circle s is mapped by a Möbius transformation M_1 to a circle $M_1(s)$ in such a way that $s \cap M_1(s) = \{m, m_{-j}\}$. Iterated application of M_1 on m and m_{-j} yields m_i, m_{2i}, \dots and m_{i-j}, m_{2i-j}, \dots

3.2. Discrete $\exp(z)$. The map $f : \mathbb{Z}^2 \rightarrow \mathbb{C}$ with $(k, l) \mapsto \exp(k + il)$ is a discrete rotational symmetric net. All quadrilaterals are similar trapezoids. Thus, $f(\mathbb{Z}^2)$ is a circular discrete holomorphic net (of conical type). We can reparametrize f in the form $(k, l) \mapsto \exp(\alpha(k) + i\beta l)$ where $\alpha : \mathbb{Z} \rightarrow \mathbb{R}$ is either strictly monotonically increasing or decreasing, and where $\beta \neq 0$ is constant. Then f is still discrete holomorphic (of conical type). It turns out (after some lengthy computations) that the cross-ratios of all quadrilaterals of the net f equal -1 if and only if $\cos \beta = 2 - \cosh(k\alpha(k) - (1+k)\alpha(1+k))$, which then implies holomorphicity in the sense of [2]. An illustration can be found in Figure 11 (bottom left).

3.3. Discrete $\exp(az)$. Before we construct a discrete $\exp(az)$ net we show the following lemma on specially defined similarities.

LEMMA 16. *Let $a_1, \dots, a_4 \in \mathbb{C}$ be four pairwise distinct points and let further S_1, S_2 be orientation preserving similarities defined by*

$$S_1(a_1) = a_4, \quad S_1(a_2) = a_3, \quad \text{and} \quad S_2(a_1) = a_2, \quad S_2(a_4) = a_3.$$

Then S_1 and S_2 commute, i.e., $S_1 \circ S_2 = S_2 \circ S_1$ (see Figure 7 left).

Proof. First, we show $S_2 \circ S_1(a_4) = S_1 \circ S_2(a_4)$. The similarities can be written in the form $S_k(z) = r_k \exp(i\varphi_k)z + u_k$ with $r_k > 0$, $\varphi_k \in [0, 2\pi)$, and $u_k \in \mathbb{C}$ for $k = 1, 2$. We have

$$\begin{aligned} S_1 \circ S_2(a_4) - S_2 \circ S_1(a_4) &= (S_1 \circ S_2(a_4) - a_3) + (a_3 - S_2 \circ S_1(a_4)) \\ &= (S_1 \circ S_2(a_4) - S_1(a_2)) + (S_2(a_4) - S_2 \circ S_1(a_4)) \\ &= r_1 \exp(i\varphi_1)(S_2(a_4) - a_2) + r_2 \exp(i\varphi_2)(a_4 - S_1(a_4)) \\ &= r_1 \exp(i\varphi_1)(S_2(a_4) - S_2(a_1)) + r_2 \exp(i\varphi_2)(S_1(a_1) - S_1(a_4)) \end{aligned}$$

$$= r_1 r_2 \exp(i(\varphi_1 + \varphi_2))(a_4 - a_1) + r_1 r_2 \exp(i(\varphi_1 + \varphi_2))(a_1 - a_4) = 0.$$

Thus, $S_2 \circ S_1(a_4) = S_1 \circ S_2(a_4)$. It is immediately clear from the definition of S_1 and S_2 that $S_2 \circ S_1(a_1) = S_1 \circ S_2(a_1)$. Consequently, both $S_1 \circ S_2$ and $S_2 \circ S_1$ are orientation preserving similarities that map the pair of two different points (a_1, a_4) to the same pair of image points $(a_3, S_1(a_3))$. Therefore, both similarities are equal. \square

PROPOSITION 17. *Let $a_1, \dots, a_4 \in \mathbb{C}$ be a quadrilateral and S_1, S_2 similarities as defined in Lemma 16. Then the net $f : \mathbb{Z}^2 \rightarrow \mathbb{C}$ with $f(k, l) = S_1^k \circ S_2^l(a_1)$ is a Koenigs net and a Koenigs lattice simultaneously.*

Proof. The proof in the case of a Koenig lattice with methods from classical projective geometry is included in the appendix.

As for the Koenigs nets we know that all quadrilaterals are similar which implies that the ratios of diagonal segments are equal for the same (combinatorial) direction of diagonals. Thus, multiplying these ratios corresponding to four faces around a vertex yields 1. All other possible cycles of diagonals can be composed by these elementary cycles which implies that the ratios of diagonal segments constitute an exact discrete multiplicative one-form. \square

PROPOSITION 18. *Let $a_1, \dots, a_4 \in \mathbb{C}$ be a circular quadrilateral and S_1, S_2 similarities as defined in Lemma 16. Then the net $f : \mathbb{Z}^2 \rightarrow \mathbb{C}$ with $f(k, l) = S_1^k \circ S_2^l(a_1)$ is a circular discrete holomorphic map (of conical type).*

Proof. A fact from elementary geometry is that a quadrilateral is circular if and only if opposite angles sum up to π . Due to the similarity construction of our net $f(\mathbb{Z}^2)$ opposite angles at a vertex are the same as opposite angles in a face (see Figure 7 center). Thus the angle condition (2) is fulfilled. The property of $f(\mathbb{Z}^2)$ being a Koenigs net/lattice follows from Proposition 17. \square

Proposition 18 yields a method to construct a few discrete holomorphic maps starting from a circular quadrilateral. We consider the following four types of circular quadrilaterals: rectangles, isosceles trapezoids, deltoids, and general (non-special) quadrilaterals.

Rectangles generate the discrete identity map from Section 3.1. *Isosceles trapezoids* generate the discrete version of $\exp(z)$ from Section 3.2. As for *general circular quadrilaterals*, they generate self-similar nets/lattices analogous to the parameter curves of $\exp(az)$. Thus, these nets/lattices can be interpreted as discrete $\exp(az)$ maps with $\operatorname{Re}(a) \cdot \operatorname{Im}(a) \neq 0$. Among those quadrilaterals the *deltoids* are symmetric and thus discretize the case where $a = \lambda(1 + i)$ for some $\lambda \in \mathbb{R} \setminus \{0\}$.

The trapezoid case is illustrated by Figure 11 (bottom left). The deltoid case is illustrated by Figure 12 (bottom left). The general quadrilateral case is illustrated by Figure 12 (bottom right).

3.4. Discrete holomorphic maps from iterated Möbius transformations.

LEMMA 19. *Let M_1 be a Möbius transformation and let s be a circle such that $s \cap M_1(s) = \{m, m_{-j}\}$ (see Figure 7 right). Let us further denote*

$$m_i = M_1(m), \quad m_{i-j} = M_1(m_{-j}), \quad m_{2i} = M_1(m_i), \quad m_{2i-j} = M_1(m_{i-j}).$$

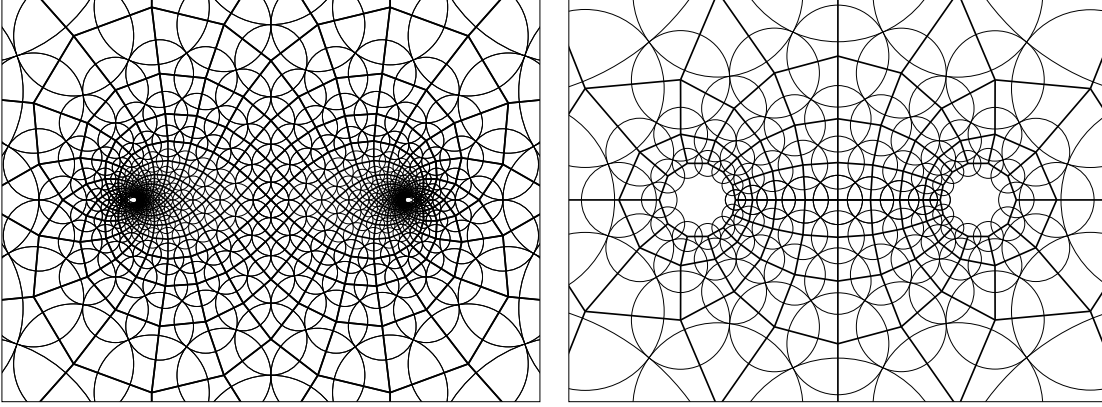


FIGURE 8. *Left:* Discrete $\tanh(az)$ with $a \in (1+i)\mathbb{R}$. *Right:* Discrete $\tanh(az)$ with $a \in \mathbb{R}$. One family of parameter curves of that type resembles electric field lines surrounding two opposite charges of the same magnitude.

We define a Möbius transformation M_2 by prescribing the following images of three points $M_2(m) = m_{-j}$, $M_2(m_i) = m_{i-j}$, $M_2(m_{2i}) = m_{2i-j}$. Then

- (a) M_1 and M_2 commute, i.e., $M_1 \circ M_2 = M_2 \circ M_1$.
- (b) M_1 and M_2 have the same fixed points.
- (c) The set of circles $s : \mathbb{Z}^2 \rightarrow \{\text{circles} \subset \mathbb{C}\}$ with $s(k, l) = M_1^k \circ M_2^l(s)$ constitute a circle pattern, meaning $s(k, l), s(k+1, l), s(k+1, l+1), s(k, l+1)$ intersect in a common point.

Proof. To prove (a) we recall the fact that any Möbius transformation is similar to a rotation and stretching, i.e., there is a Möbius transformation M such that $M^{-1} \circ M_1 \circ M(z) = wz$ for some $w \in \mathbb{C}$. Consequently, w.l.o.g. we can assume that M_1 is a similarity. Lemma 16 implies that the orientation preserving similarity S_2 defined by $S_2(m) = m_{-j}$ and $S_2(m_i) = m_{i-j}$, also maps m_{2i} to m_{2i-j} . Consequently, $M_2 = S_2$ and in particular Lemma 16 implies that M_1 and M_2 commute.

The fact that any two Möbius transformations that are different from the identity have the same fixed points if and only if they commute proves (b). For a proof of that fact consider again first the special case $M_1(z) = wz$ with $w \in \mathbb{C}$.

Statement (c) follows immediately from the definition of the Möbius transformations M_1, M_2 and from (a). \square

Note that the Möbius transformation M_2 not only depends on M_1 but also on the choice of the circle s .

PROPOSITION 20. *Let M_1, M_2 be Möbius transformations as defined in Lemma 19. Then the centers of the circle pattern $s : \mathbb{Z}^2 \rightarrow \{\text{circles} \subset \mathbb{C}\}$ with $s(k, l) = M_1^k \circ M_2^l(s)$ constitute a (not necessarily circular) discrete holomorphic map f (of conical type).*

Proof. The proof follows immediately from Lemma 19, Proposition 18, and the fact that any Möbius transformation is similar to a rotation and stretching of the form $z \mapsto wz$ with $w \in \mathbb{C}$. \square

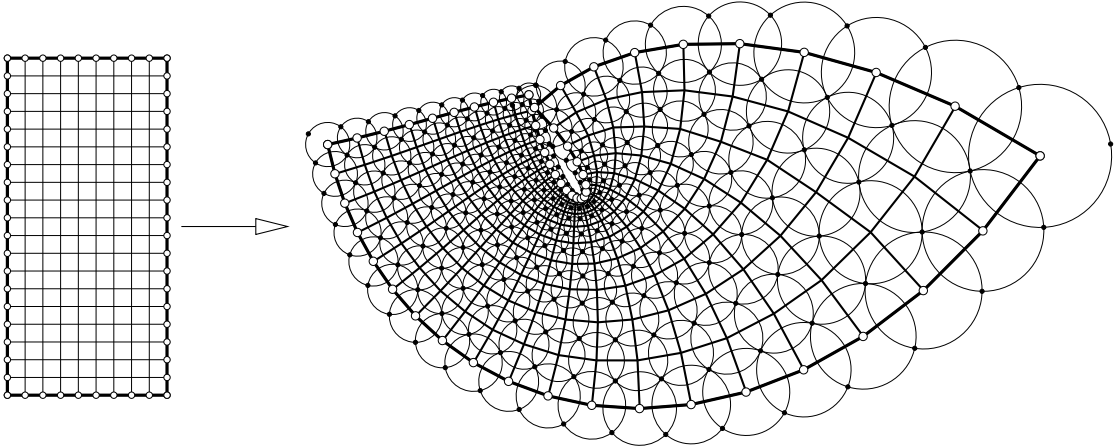


FIGURE 9. Illustration of the discrete Riemann mapping described in Section 3.6. This figure is a solution of a non-linear numerical optimization approach and has no rigorous proof.

A discrete holomorphic nets $f(\mathbb{Z}^2)$ from Proposition 20 as iterated Möbius transformations is illustrated by Figure 8 (left). Note that in general these nets $f(\mathbb{Z}^2)$ are not circular.

3.5. Discrete $\tanh(az)$. There is the following representation of the smooth hyperbolic tangent function in terms of the exponential function: $\tanh(az) = \frac{\exp(2az)-1}{\exp(2az)+1}$. Thus, to obtain a discrete $\tanh(az)$ we apply the Möbius transformation $z \mapsto \frac{z-1}{z+1}$ to a discrete net discretizing $\exp(2az)$ from Section 3.3. For an illustration see Figure 8 (right).

3.6. Discrete Riemann mapping (experiment). The result of this paragraph is only motivated by counting degrees of freedom and numerical experiments. The classical Riemann mapping theorem says that there is a biholomorphic map between any open and simply connected domain in \mathbb{C} (but not the plane itself) and the open unit disc.

We try to interpret the Riemann mapping theorem in our discrete setting. To that end we prescribe a closed polygon in \mathbb{C} which is combinatorial equivalent to the border of the lattice $\{0, \dots, m\} \times \{0, \dots, n\}$. Now we ask the following question. Is it possible to find a discrete holomorphic map (of conical type) that coincides with the given border polygon. We don't have a rigorous answer to that question but we make the following observation. For the moment we only consider Koenigs nets (i.e., in the sense of [4]). We have $m \times n$ inner points and consequently $m \times n \times 2$ degrees of freedom for choosing them. On the other hand we have two conditions on each inner vertex star to be fulfilled to be a discrete holomorphic map namely the angle condition (2) and the Koenigs condition. That is, we also have $m \times n \times 2$ conditions. From this considerations we suspect the existence of a unique discrete holomorphic map solving the given initial value problem. An illustration of this discrete Riemann mapping can be found in Figure 9.

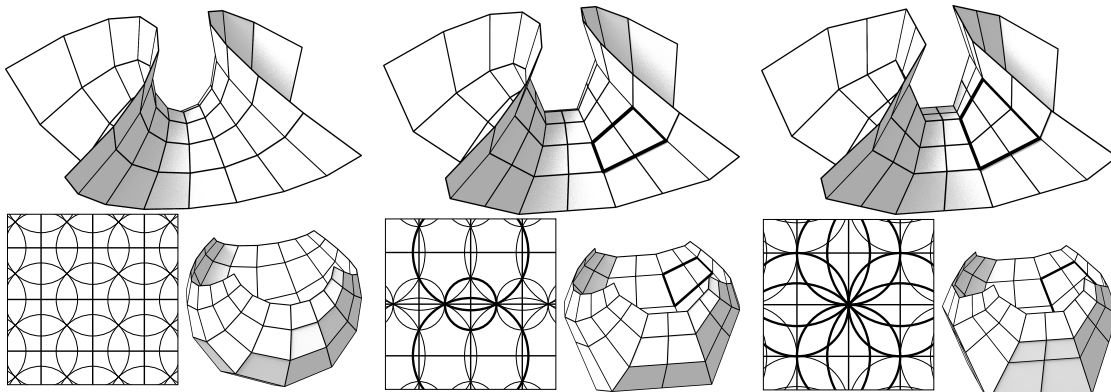


FIGURE 10. Enneper's minimal surface and the influence of the underlying circle pattern. For details see Section 4.1.

4. DISCRETE MINIMAL SURFACES

Generating discrete minimal surfaces in \mathbb{R}^3 from isothermic parametrizations of a sphere via discrete analogues of the Christoffel transformation is by now a well established theory [1–3, 11, 13, 15]. We take advantage of that theory to generate conical minimal surfaces in the following way. We start with a discrete holomorphic map (of conical type) f in \mathbb{C} , where we restrict ourselves to Koenigs nets (i.e., in the sense of [4]). Then we construct one instance s of the family of underlying circle patterns and stereographically project the associated circles to the sphere. Then we construct the poles of the supporting planes of the circles with respect to the sphere. In other words we consider the spherical model of Sec. 2.3.2. Cor. 12(a) guarantees that the so generated net is a conical Koenigs net, i.e., a discrete isothermic net. Then we apply the Christoffel dual transformation (1) to obtain *discrete minimal surfaces* (of conical type).

4.1. Discrete Enneper's surface. Three versions of a discrete Enneper's minimal surface are depicted in Figure 10. The discrete holomorphic map corresponding to Enneper's minimal surface is the discrete identity, i.e., in our case we take a scalar multiple of the \mathbb{Z}^2 grid. In all three images there is the minimal surface and beneath the corresponding holomorphic map with underlying circle pattern and the Gauss image. The natural way to choose an underlying circle pattern is to take the centers of the squares as intersection points m of the four circles corresponding to that square as in Figure 10 (left). In Figure 10 (center) the points m are now centers of horizontal edges. The symmetry of the net implies that the three highlighted circles are in the same pencil of circles. Thus, the corresponding lifted points of the spherical model (which is our Gauss image) of these three circles are collinear. Consequently, in the minimal surface there are pairs of adjacent quadrilaterals which lie in the same plane. In Figure 10 (right) the points m are coincident with vertices of the holomorphic data. Thus, there is always one circle corresponding to each face in the underlying circle pattern that degenerates to a point. Consequently, all nine circles corresponding to all four faces around m pass through m , which implies coplanarity of these four faces in the Gauss image as well as in the minimal surface.

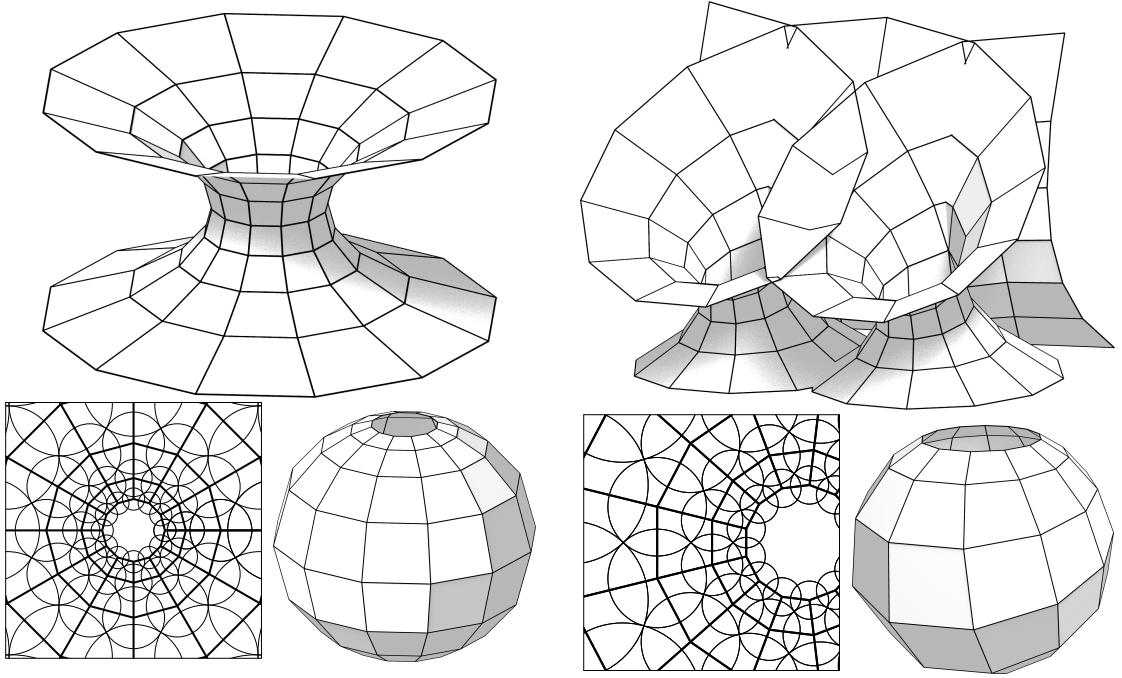


FIGURE 11. Discrete catenoid (left) and a Goursat transformation of a discrete catenoid (right) together with holomorphic data and Gauss image.

4.2. Discrete catenoid and its Goursat transformation. Figure 11 (left) illustrates a discrete catenoid. The corresponding holomorphic data is the discrete $\exp(z)$ function. We obtain the specific holomorphic net for Figure 11 by taking a rotational symmetric quadrilateral and construct a net by applying Proposition 18. Elementary geometric considerations imply that the points of intersection of diagonals can be taken as points $m : \mathbb{Z}^2 \rightarrow \mathbb{C}$. Convergence of this version of the discrete catenoid to its smooth counterpart has been considered in [14].

A *Goursat transformation* of an isothermic parametrization f of a minimal surface is defined by $(M \circ f^*)^*$, where M is a Möbius transformation and where f^* denotes the Christoffel dual of f (see Equation (1)). That is, a Goursat transformation is the dual of a net obtained by a Möbius transformation applied to the dual of f . For more details on Goursat transformations see e.g., [11, Sec. 5.3]. For Figure 11 (right) we just used $\exp(z) + c$, i.e., a translation of the holomorphic net of Figure 11 (left), and we run through the original catenoid twice.

4.3. Discrete helicoid and helicoidal minimal surfaces. The holomorphic data of the smooth helicoid is of the form $\exp((1+i)z)$. The isothermic parametrization of the helicoid is clearly not the same as the more common one that we get by applying a helical motion to a straight line that intersects the central axis orthogonally. Figure 12 (left) illustrates a discrete version of that surface. The map discretizing $\exp((1+i)z)$, that we considered in Section 3.3, is generated by applying Proposition 18 to a circular

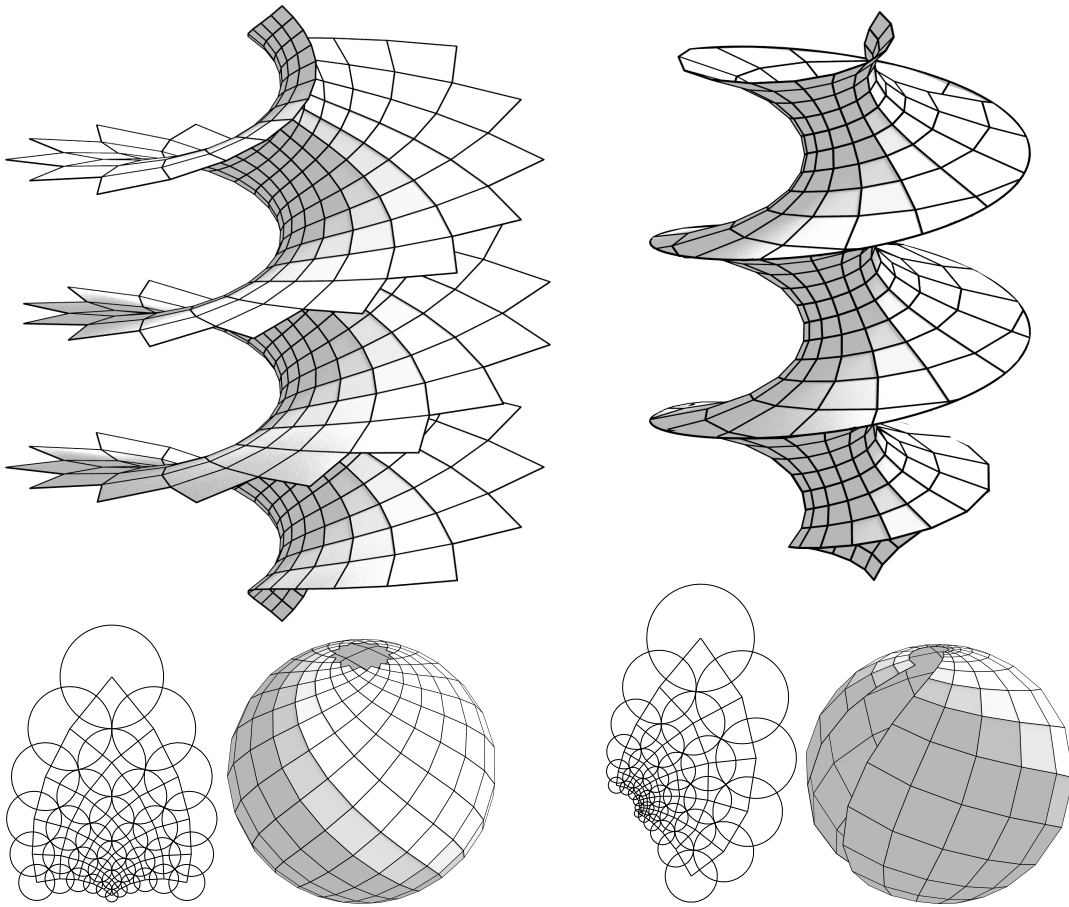


FIGURE 12. A discrete helicoid (left) and a discrete helical minimal surface (right) together with holomorphic data and Gauss image.

deltoid. We only depict a small part of the discrete holomorphic map because the entire net would overlap and destroy the significance of the image.

Helicoidal minimal surfaces are studied e.g., in [23]. Those are contained in the associated family in which both the catenoid and the helicoid appear. The corresponding holomorphic data is the function $z \mapsto \exp(az)$ with $a \in \mathbb{C} \setminus (\mathbb{R} \cup (1+i)\mathbb{R})$. Figure 12 (right) illustrates a discrete helical minimal surface. For the illustration we trimmed the surfaces at their self intersections. The discrete analogue of $\exp(az)$ is generated by applying Proposition 18 to a non-symmetric circular quadrilateral as explained in Section 3.3. Figure 12 (right) only illustrates a part of the discrete holomorphic map and of the Gauss image.

APPENDIX

In the appendix we give a proof of Proposition 17 with methods from classical projective geometry. We split up the proof into the following lemmas. For further details on projective geometry see e.g. the textbook [18].

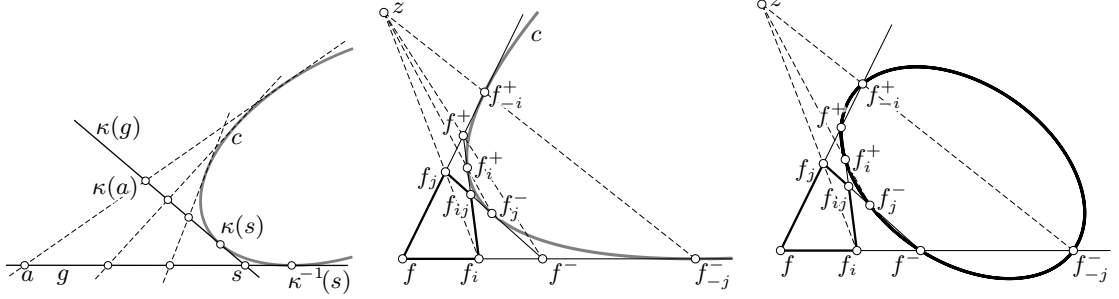


FIGURE 13. Illustrations of Lemma 21 (left), Lemmas 22 and 23 (center), and proof of Proposition 17 (right).

LEMMA 21. Let $\kappa : \mathbb{P}^2 \rightarrow \mathbb{P}^2$ be a collineation in the real projective plane \mathbb{P}^2 , and let g denote a straight line. Furthermore, let us denote the point of intersection of the line g and $\kappa(g)$ by s (see Figure 13 left). Then the conic c that is tangent to all lines $a \vee \kappa(a)$ for all $a \in g$ (J. Steiner's definition of line-conics) touches both lines g and $\kappa(g)$ at $\kappa^{-1}(s)$ and $\kappa(s)$, respectively.

Proof. g and $\kappa(g)$ are in the set of lines tangent to c . Let us assume c touches g in a point t different from $\kappa^{-1}(s)$. According to our definition of c the straight line h connecting t and $\kappa(t) \neq s$ is a tangent of c . However, it is impossible to have two different tangents g and h both going through t . The proof for $\kappa(s)$ being a contact point works analogously. \square

LEMMA 22. Let $f, f_i, f_{ij}, f_j \in \mathbb{P}^2$ be four points and let further S_1, S_2 be orientation preserving similarities defined by (for notation cf. Section 1.3 and Figure 13 center)

$$S_1(f) = f_j, \quad S_1(f_i) = f_{ij}, \quad \text{and} \quad S_2(f) = f_i, \quad S_2(f_j) = f_{ij}.$$

Furthermore, let

$$\begin{aligned} f^- &= (f \vee f_i) \cap (f_j \vee f_{ij}), & f^+ &= (f \vee f_j) \cap (f_i \vee f_{ij}), \\ f_{-j}^- &= S_1^{-1}(f^-), & f_{-i}^+ &= S_2^{-1}(f^+), \\ f_j^- &= S_1(f^-), & f_i^+ &= S_2(f^+). \end{aligned}$$

Then there is a conic c tangent

$$\begin{aligned} (6) \quad & \text{to } f \vee f_i \text{ at } f_{-j}^-, & & \text{to } f_j \vee f_{ij} \text{ at } f_j^-, \\ (7) \quad & \text{to } f \vee f_j \text{ at } f_{-i}^+, & & \text{to } f_i \vee f_{ij} \text{ at } f_i^+. \end{aligned}$$

Proof. There is a conic c constructed with Lemma 21 for the collineation $\kappa = S_1$ and for $g = f \vee f_i$. Consequently, by construction (6) is fulfilled and the four connecting lines from (6) and (7) are tangent to c . Since S_1 is a similarity one tangent of c is the line at infinity. Consequently, c is the unique parabola tangent to the four lines from (6) and (7). Analogously, S_2 produces a parabola fulfilling (7) and having the same four tangents as c . Therefore the second conic is identically equal to c . \square

LEMMA 23. *We take the same assumptions and notations as in Lemma 22. Then the four lines*

$$f_i \vee f_j, \quad f^- \vee f^+, \quad f_j^- \vee f_i^+, \quad f_{-j}^- \vee f_{-i}^+,$$

all pass through a common point z . For an Illustration see Figure 13 (center).

Proof. We apply Brianchon's theorem (see e.g., [18, Th. 10.7]) two times.

First, we consider the two line elements (i.e., tangent plus contact point) $t_{12} = (f_j \vee f_{ij}, f_j^-)$, $t_{45} = (f_i \vee f_{ij}, f_i^+)$ and the two tangents $t_3 = f \vee f_j$ and $t_6 = f \vee f_i$. Brianchon's theorem stays true if we replace two different tangents by one line element. That is, two tangents t_1, t_2 can be replaced by one line element (t_{12}, T) where $t_1 \cap t_2$ then corresponds to the contact point T . Brianchon's theorem now implies that the three lines

$$\begin{aligned} (t_1 \cap t_2) \vee (t_4 \cap t_5) &= f_j^- \vee f_i^+, \\ (t_2 \cap t_3) \vee (t_5 \cap t_6) &= f_j \vee f_i, \\ (t_3 \cap t_4) \vee (t_6 \cap t_1) &= f^+ \vee f^-, \end{aligned}$$

pass through a common point z . Analogously, for the two line elements $t_{12} = (f \vee f_i, f_{-j}^-)$, $t_{45} = (f \vee f_j, f_{-i}^+)$ and the two tangents $t_3 = f_i \vee f_{ij}$ and $t_6 = f_j \vee f_{ij}$ we obtain, by applying Brianchon's theorem, that the three lines

$$\begin{aligned} (t_1 \cap t_2) \vee (t_4 \cap t_5) &= f_{-j}^- \vee f_{-i}^+, \\ (t_2 \cap t_3) \vee (t_5 \cap t_6) &= f_i \vee f_j, \\ (t_3 \cap t_4) \vee (t_6 \cap t_1) &= f^+ \vee f^-, \end{aligned}$$

pass through a common point \tilde{z} . However, z and \tilde{z} is the same point since both lines $f_i \vee f_j$ and $f^+ \vee f^-$ are in both sets of lines. \square

Now we have collected all the properties we need to prove Proposition 17.

of Proposition 17. By applying Pascals theorem (see e.g., [18, Th. 10.6]) we show the existence of a conic passing through $p_1 = f_{-i}^+$, $p_2 = f^+$, $p_3 = f_i^+$, $p_4 = f_j^-$, $p_5 = f^-$, $p_6 = f_{-j}^-$. Lemma 23 implies that the three points

$$(p_1 \vee p_2) \cap (p_4 \vee p_5) = f_j, \quad (p_2 \vee p_3) \cap (p_5 \vee p_6) = f_i, \quad (p_3 \vee p_4) \cap (p_6 \vee p_1) = z,$$

are collinear (see Figure 13 right). Consequently, Pascal's theorem implies that the six points p_1, \dots, p_6 lie on a conic. \square

ACKNOWLEDGEMENTS

This research was supported in part by the DFG Collaborative Research Center TRR 109, 'Discretization in Geometry and Dynamics' through grant I 706-N26 of the Austrian Science Fund (FWF).

REFERENCES

- [1] Alexander I. Bobenko, Tim Hoffmann, and Boris A. Springborn. Minimal surfaces from circle patterns: geometry from combinatorics. *Ann. of Math. (2)*, 164(1):231–264, 2006.
- [2] Alexander I. Bobenko and Ulrich Pinkall. Discrete isothermic surfaces. *J. Reine Angew. Math.*, 475:187–208, 1996.
- [3] Alexander I. Bobenko and Yuri B. Suris. *Discrete differential geometry: Integrable Structure*. Number 98 in Graduate Studies in Math. American Math. Soc., 2008.
- [4] Alexander I. Bobenko and Yuri B. Suris. Discrete Koenigs nets and discrete isothermic surfaces. *Int. Math. Res. Not. IMRN*, (11):1976–2012, 2009.
- [5] Thomas E. Cecil. *Lie sphere geometry*. Universitext. Springer, New York, second edition, 2008.
- [6] Elwin Bruno Christoffel. Ueber einige allgemeine Eigenschaften der Minimumsflächen. *J. Reine Angew. Math.*, 67:218–228, 1867.
- [7] Gaston Darboux. *Leçons sur la théorie générale des surfaces et les applications géométriques du calcul infinitésimal. Deuxième partie*. Chelsea Publishing Co., Bronx, N.Y., 1972.
- [8] Adam Doliwa. Geometric discretization of the Koenigs nets. *J. Math. Phys.*, 44(5):2234–2249, 2003.
- [9] Zheng-Xu He and Oded Schramm. On the convergence of circle packings to the Riemann map. *Invent. Math.*, 125(2):285–305, 1996.
- [10] Peter Henrici. *Applied and computational complex analysis. Vol. 1-3*. Wiley Classics Library. John Wiley & Sons Inc., New York.
- [11] Udo Hertrich-Jeromin. *Introduction to Möbius differential geometry*, volume 300 of *London Mathematical Society Lecture Note Series*. Cambridge University Press, Cambridge, 2003.
- [12] Yang Liu, Helmut Pottmann, Johannes Wallner, Yong-Liang Yang, and Wenping Wang. Geometric modeling with conical meshes and developable surfaces. *ACM Trans. Graphics*, 25(3):681–689, 2006. Proc. SIGGRAPH.
- [13] Christian Müller. Conformal hexagonal meshes. *Geom. Dedicata*, 154:27–46, 2011.
- [14] Christian Müller. Discretizations of the hyperbolic cosine. *Beitr. Algebra Geom.*, 54(2):509–531, 2013.
- [15] Christian Müller and Johannes Wallner. Semi-discrete isothermic surfaces. *Results Math.*, 63(3-4):1395–1407, 2013.
- [16] Helmut Pottmann and Yang Liu. Discrete surfaces in isotropic geometry. In *IMA Conference on the Mathematics of Surfaces*, volume 4647 of *Lecture Notes in Computer Science*, pages 341–363. Springer, 2007.
- [17] Helmut Pottmann and Johannes Wallner. The focal geometry of circular and conical meshes. *Adv. Comput. Math.*, 29(3):249–268, 2008.
- [18] Jürgen Richter-Gebert. *Perspectives on projective geometry*. Springer, Heidelberg, 2011.
- [19] Burt Rodin and Dennis Sullivan. The convergence of circle packings to the Riemann mapping. *J. Differential Geom.*, 26(2):349–360, 1987.
- [20] Robert Sauer. *Differenzgeometrie*. Springer-Verlag, Berlin, 1970.
- [21] Kenneth Stephenson. *Introduction to circle packing*. Cambridge University Press, Cambridge, 2005.
- [22] Wenping Wang, Johannes Wallner, and Yang Liu. An angle criterion for conical mesh vertices. *J. Geom. Graph.*, 11(2):199–208, 2007.
- [23] Walter Wunderlich. Beitrag zur Kenntnis der Minimalschraubflächen. *Compositio Math.*, 10:297–311, 1952.

INSTITUTE OF DISCRETE MATHEMATICS AND GEOMETRY, VIENNA UNIVERSITY OF TECHNOLOGY.
 WIEDNER HAUPTSTRASSE 8-10/104, 1040 VIENNA EMAIL: CMUELLER@GEOMETRIE.TUWIEN.AC.AT